2023-05

Physical and biogeochemical controls on seasonal iron, manganese, and cobalt distributions in Northeast Atlantic shelf seas

Chen, X-G

10.1016/j.gca.2023.03.023
Geochimica et Cosmochimica Acta
Elsevier

Ocean circulation and biological cycles drive seasonal variations of dissolved Al, Cd, Ni, Cu, and Zn on the Northeast Atlantic continental margin

Xue-Gang Chen[1,2*#], Dagmara Rusiecka[1,3#], Martha Gledhill[1,3], Angela Milne[4], Amber L. Annett[3], Aaron Joseph Beck[1], Antony Birchill[4], Maeve Lohan[3], Simon Ussher[4], Eric P. Achterberg[1,3*]

[1] GEOMAR Helmholtz Centre for Ocean Research Kiel, Kiel, Germany,

[2] Ocean College, Zhejiang University, Zhoushan, China

[3] Ocean and Earth Sciences, National Oceanography Centre, University of Southampton, Southampton, UK

[4] School of Geography, Earth and Environmental Sciences, University of Plymouth, Plymouth, UK

Corresponding authors:

Xue-Gang Chen, xchen@geomar.de, chenxg83@zju.edu.cn

Eric P. Achterberg, eachterberg@geomar.de

Both authors contribute equal to this paper.

Key Points:

- Seasonal cycles of biological processes and fluvial inputs drive dissolved trace metal variations in surface waters of Northeast (NE) Atlantic continental margin.
- Dissolved Al, Cd, Ni, Cu, and Zn concentrations and metal:P ratios at depth are controlled by the mixing of different water masses.
- Mediterranean outflow waters provide a strong imprint on distributions of dissolved trace metals and metal:P ratios in the NE Atlantic Ocean.

Abstract

We report the seasonal distributions of dissolved zinc (dZn), nickel (dNi), copper (dCu), cadmium (dCd), aluminum (dAl), and nutrients (nitrate+nitrite (TN), phosphate (P), and silicic acid (Si), as well as their relationships on the Northeast (NE) Atlantic continental margin (Celtic Sea). Along the continental slope, surface dissolved trace metal (dTM) and nutrient concentrations were controlled by seasonal cycling of enhanced phytoplankton uptake in summer, remineralization of organic particles in autumn, and strong mixing in winter. Water columns on the shelf received additional impact from a zero-salinity endmember, e.g., fluvial input from the British Isles. The balance between fluvial input (especially for dCu and dZn) and seasonal cycling of biogeochemical processes resulted in highly variable dTM:nutrient stoichiometry across the shelf. Distributions of dTMs and nutrients at depth on the slope were regulated by the water mass mixing driven by ocean circulation without invoking local remineralization process. The Mediterranean Outflow Waters are especially important to transport Mediterranean-sourced dTMs (e.g., dAl, dZn, and dNi) into the NE Atlantic Ocean and drive dAl:P and dCu:P kinks at a depth of ~ 1000 m. These results highlight the importance of riverine input and ocean circulation on the seasonal distributions of nutrients and nutrient-like dTMs in temperate continental margins, which could further affect local biological carbon pump.

Plain Language Summary

1. Introduction

Dissolved (< 0.2 μm) trace metals (dTMs) including zinc (Zn), nickel (Ni), copper (Cu) and perhaps cadmium (Cd), are important micronutrients in marine systems. Low supply of dTMs could potentially affect marine ecosystem structure and functioning (Lohan & Tagliabue, 2018; Morel & Price, 2003; Twining & Baines, 2013). Specifically, Zn is connected to a series of proteins, e.g., carbonic anhydrase and alkaline phosphatase, and Zn availability can influence access of phytoplankton to the dissolved organic phosphorus pool (Lohan & Tagliabue, 2018;

Mahaffey et al., 2014). Nickel is primarily associated with urease, and superoxide dismutase has a Ni-containing form. Copper is used in photosynthetic and respiratory electron transport chains (La Fontaine et al., 2002; Twining & Baines, 2013). Cadmium can substitute Zn in carbonic anhydrase in diatoms (Lane et al., 2005; Lane & Morel, 2000), or rather, Cd is mistakenly assimilated into micro-organic cells with other divalent metals (Horner et al., 2013). Due to their close association with biological activities, dissolved Zn (dZn), Ni (dNi), Cu (dCu) and Cd (dCd), are classified as biogenic dTMs (bdTMs) and their vertical distributions resemble those of nutrients (Nitrate+Nitrite (TN), phosphate (P), and silicic acid (Si)) (Bruland et al., 2014; Lohan & Tagliabue, 2018). These dTMs typically exhibit seasonal depleted concentrations in surface waters due to phytoplankton uptake (C. M. Moore et al., 2013; Morel & Price, 2003), and elevated levels at depth due to remineralization of sinking organic particles (Boyd et al., 2017; Bruland et al., 2014). Nutrient and bdTMs, therefore, show significant positive correlations with as examples the dCd-P relationships in the global ocean (Boyle et al., 1976; Boyle, 1988; Middag et al., 2018; Roshan & Wu, 2015; Wu & Roshan, 2015; Xie et al., 2015), dZn-P correlations in the South Atlantic Ocean (Wyatt et al., 2014) and Southern Ocean (Saito et al., 2010), and dNi-P and dCu-Si correlations in the Southern Ocean (e.g., Janssen et al., 2020).

However, the linear relationships between bdTMs and nutrients usually show pronounced changes in slopes, e.g., P of ~ 1.3 μM for Cd:P correlation (de Baar et al., 1994; Cullen, 2006; Middag et al., 2018). The origin of such kinks (especially the Cd:P kink) has been scientifically debated over the last decades. Some hypotheses point towards deeper regeneration of Cd relative to P (Boyle, 1988; Roshan & DeVries, 2021), or enhanced Cd uptake due to the limitation of bio-essential elements in surface waters (Cullen, 2006; Sunda & Huntsman, 2000). Kinks were also assigned to a chemical replacement between Co, Zn, and Cd in carbonic anhydrase (Morel et al., 1994; Price & Morel, 1990) or a change in bioavailability of Cd through organic complexation (Bruland, 1992). Recent studies demonstrated that the mixing of water masses with different Cd:P ratios could be a dominant factor accounting for the observed kinks (Baars et al., 2014; Middag et al., 2018; Xie et al., 2015). In addition, external sources such as continental inputs and dust deposition (Menzel Barraqueta et al., 2018; Middag et al., 2022), that can be traced by dissolved aluminum (dAl) inputs (Han et al., 2008; Measures & Edmond, 1988), can affect bdTM distributions in the ocean. Since there is a continued debate surrounding the drivers underpinning

bdTM distributions, further investigations regarding the occurrences of nutrients and bdTMs as well as their relationships are crucial for understanding biogeochemical cycles in paleo – and modern oceans.

Continental margins with their shelves and slopes are junctions between terrestrial systems and the ocean. The disproportionately high primary production and particulate organic carbon export make continental margins important transition zones for the marine carbon cycle (Muller-Karger et al., 2005; Simpson & Sharples, 2012; Zhang et al., 2019). Here, we report on the seasonal distributions of bdTMs, dAl, and nutrients on the Northeast (NE) Atlantic continental margin (Celtic Sea), which is characterized by large seasonal variations of biological activities (Birchill et al., 2017), a complex bathymetry and a dynamic water circulation (Fig. 1a). A high sampling resolution (Fig. 1b) offers us an ideal opportunity to study the influence of terrestrial inputs, biogeochemical processes and ocean circulation on the seasonal variations of bdTMs and their relationships with nutrients in this system.

2. Methods

The sampling procedures have been reported in detail by Rusiecka et al. (2018). We conducted one transect on the continental shelf of the Celtic Sea, from Station A near the Bristol channel to station CS2 near the shelf break (Fig. 1b). Two off-shelf transects were conducted along a canyon (stations Fe01 - Fe07, Fe15) and a spur (stations Fe08 - Fe14) (Fig. 1b). Samples were collected on board the *RRS Discovery* during three different seasons: an autumn cruise in November 2014 (DY018), a spring cruise in April 2015 (DY029), and a summer cruise in July 2015 (DY033).

Seawater samples for dTM analyses were collected following GEOTRACES protocols (Cutter et al., 2017). Samples were filtered immediately upon collection using a 0.2 μm filter capsule (Acropack). Trace metals were pre-concentrated at GEOMAR using an automated system (SC-4 DX SeaFAST pico; ESI) and analyzed by high-resolution inductively coupled plasma mass spectrometry (HR-ICP-MS, Thermo Fisher Element XR) as per Rapp et al. (2017). Dissolved Al concentrations were analyzed by a spectrofluorometer (Cary Eclipse) as per Hydes & Liss (1976). Short-lived radium (Ra) isotopic activities, ^{223}Ra (half-life, $t_{1/2}$ = 11.4 days) and ^{224}Ra (half-life,

$t_{1/2}$ = 3.66 days), were counted from large volume samples using a Radium Delayed Coincidence Counter (W. S. Moore, 2008). Radium isotope activities here are reported in excess of activity supported by their parent isotopes in the water column. Nutrients, P, Si, and TN, were measured on board using techniques described in Woodward & Rees (2001), according to the International GO-SHIP nutrient manual recommendations (Hydes et al., 2010). Further details can be found in the supporting information.

3. Results and discussion

Dissolved Cd, Zn, Ni, and Cu exhibited nutrient-like vertical distributions during all seasons on the NE Atlantic continental margin (Fig. 2, Fig. 3), with the lowest concentrations observed in surface waters due to biological utilization, and elevated concentrations at depth ascribed to remineralization (Bruland et al., 2014; C. M. Moore et al., 2013). The canyon and spur transects showed identical vertical profiles for dTMs and nutrients across all seasons. In the following section, both transects on the slope were combined as a slope transect. While the deep bdTM and nutrient concentrations on the continental slope were relatively constant throughout the year, surface bdTM and nutrient levels on the continental shelf and slope showed pronounced seasonal variations (Table S2, Fig. S2, Fig. S3). Kinks in dTM:nutrient ratios (e.g., dZn:P and dCu:P) ratios were observed on the continental slope at a depth of ~ 100 m and ~ 1000 m (Fig. S4). The shelf seas showed higher dCu, dNi, dZn, and Si concentrations than those on the slope (Fig. 3), accompanied by varying dTM: nutrient correlations (Fig. S5).

3.1 Biological influence on seasonal variations in surface dTM concentrations along the continental slope

A seasonal mixed layer (SML) covers the continental slope with a depth of ~ < 100 m fron spring to autumn (Supporting information: Hydrography). A reduction in dTM and nutrient levels in the SML (especially at depths < 30 m) was observed between April 2015 and July 2015, due to biological utilization and water column stratification (Birchill et al., 2017) (Fig. S6, Table S2). The total drawdown of surface (depth < 30 m) dTMs and nutrients on the slope from April to July were: dAl 2.68 ± 2.25 nM, dCd 79.5 ± 45.1 pM, dCu 0.08 ± 0.11 nM, dNi, 0.67 ± 0.31 nM, dZn

0.10 ± 0.25 nM, P 0.35 ± 0.11 μM, TN 6.71 ± 1.83 μM, and Si 2.44 ± 0.47 μM (Table S2). The fraction of Cd, Ni, and TN removed over this period on the slope was higher, and drawdown of Cu was lower than reported for the study region between January 1994 and June 1995 (36% TN, 41% Cd, 22% Cu, 14% Ni) (Cotté-Krief et al., 2002) and March – June 1987 (56% Cd, 12% Cu, 4% Ni) (Kremling & Pohl, 1989). The decrease in dTM and nutrient concentrations was the consequence of phytoplankton uptake in summer, and the overall "uptake" ratio of phytoplankton normalized to P was:

$$(N_{19}Si_{7}P_{1})_{1000}Al_{7.5}Ni_{1.9}Zn_{0.34}Cu_{0.23}Cd_{0.23}$$

The surface dTM and nutrient concentrations on the continental slope increased from July to November, accompanied by comparable correlations between dTMs/nutrients and AOU at 20 – 100 m (Fig. S7). Hence, the increase in surface dTM and nutrient concentrations in November was attributed to the remineralization of organic particles (Anderson & Sarmiento, 1994; Lohan & Tagliabue, 2018). Both surface and deep waters showed similar dTMs/nutrients – AOU correlations in April, likely reflecting water column mixing in winter (Fig. S7). Therefore, the increase in surface dTM and nutrient concentrations from November to April was attributed to resupply from subsurface waters. Using concentration differences between July and November (Table S2), we estimated the apparent "remineralization" ratio of dTMs and nutrients normalized to P as:

$$(N_{15}Si_{6}P_{1})_{1000}Al_{10.7}Ni_{1.9}Zn_{0.56}Cu_{0.49}Cd_{0.28}$$

and the "winter mixing" ratio estimated from the concentration differences between November and April observations as:

$$(N_{21}Si_{7.5}P_{1})_{1000}Al_{5.4}Ni_{1.8}Zn_{0.19}Cu_{0.06}Cd_{0.19}$$

The estimated Zn:P and Cu:P ratios between "uptake" and "remineralization" , but the "winter mixing" ratios varied strongly from these ratios, probably due to a relatively limited seasonal variations and large concentration ranges of both metals (Fig. S6; Table S2). The N:P, Si:P, Ni:P, and Cd:P ratios were relatively constant, indicating a close association of Ni and Cd with biological processes in surface waters across all seasons. The observed "uptake", "remineralization", and "winter mixing" ratios are close to the overall dTM:P ratios in the SML (depth of < ~ 100 m) (dAl:P of 8.68 mmol mol^{-1}, dCd:P of 214 μmol mol^{-1}, dCu:P of 0.199 mmol mol^{-1}, dNi:P of 1.53 mmol mol^{-1}, and dZn:P of 0.37 mmol mol^{-1}) (Table S3). The dTM:P ratio

here is broadly consistent with metal:P ratios observed in full depth profiles in the North Atlantic Ocean (Zn:P of 2.6 ± 1.0 mmol mol^{-1}, Ni:P of 1.6 ± 0.1 mmol mol^{-1}, Cu:P of 0.30 mmol mol^{-1}, and Cd:P of 0.24 ± 0.12 mmol mol^{-1}) (Middag et al., 2018; Twining & Baines, 2013 and references therein) and the extended Redfield ratio of phytoplankton cultures (Zn:P of 0.80 mmol mol^{-1}, Cu:P of 0.38 mmol mol^{-1}, and Cd:P of 0.21 mmol mol^{-1}) (Ho et al., 2003). Therefore, the positive correlations between dTMs and nutrients in the SML on the continental slope across all seasons (Fig. S4) generally reflected the seasonal cycling of biological uptake in summer, remineralization of organic particles in autumn, followed by winter mixing.

3.2 Additional fluvial inputs of dTMs on the continental shelf

Seasonal cycling of biological processes also affected the dTM and nutrient distributions on the continental shelf of the NE Atlantic Ocean. Using station CCS (central Celtic Sea) as an example (Fig. S8), surface dTM and nutrient concentrations decreased from April to July due to phytoplankton uptake and slightly increased from July to November due to remineralization. The gradually increase in nutrient concentrations from April to November at depths > 50 m was attributed to the remineralization of sinking organic particles (Birchill et al., 2017; Lohan & Tagliabue, 2018). Unlike similar dTM:P ratios at all stations on the slope, the overall dTM:P ratios on the shelf varied greatly between sampling locations (Fig. S9). These variations were accompanied by gradually decreasing dTM concentrations with increasing distance offshore (Fig. S10), suggesting the dTM stocks on the shelf were determined by external sources. Benthic sediments were likely not an important source for the enhanced dTMs, since dTM concentrations did not change significantly with $^{223}Ra_{xs}$ and $^{224}Ra_{xs}$ activities (Fig. S11) which indicates minimal benthic TM supply.

Instead, a decreasing salinity with increasing distance offshore (Fig. 3) and strong negative correlations between dTMs (especially for dAl, dCu, dNi, and dZn) and salinity suggest dTM distributions on the shelf (Fig. S12) were augmented by a dTM-rich zero-salinity endmember e.g., riverine input from the British Isles through Irish Sea and/or the Bristol channel (Achterberg et al., 1999; Kremling & Hydes, 1988). Based on the correlations between subsurface (depth of 50 – 200 m to exclude surface biological activities) dTMs, nutrients, and salinity in April when significant correlations were observed, the apparent endmember concentrations of the freshwater

endmember at salinity of 0 were calculated as: dCd, 139 ± 1202 pM; dCu, 214 ± 26 nM; dNi, 26.1 ± 22.7 nM; dZn, 392 ± 63 nM; TN, 59.4 ± 79.2 μM; P, 6.15 ± 4.67 μM; and Si, 192 ± 37 μM. The enrichment of dCu, dZn, and Si relative to P in the fluvial endmember caused gradually decreasing dCu:P and dZn:P ratios with increasing distance stretching from station A to CS2 (Fig. S9). Fluvial input was not a major source of dCd and dNi, thereby resulting in increasing dCd:P and dNi:P ratios with offshore distance. At station CS2, the dTM:P, TN:P, and Si:P ratios were close to those on the continental slope.

The salinity in subsurface waters at station A gradually increased from ~ 34.9 in April to ~ 35.3 in November (Fig. 3), suggesting gradually decreasing fluxes of riverine waters or an increasing contribution of North Atlantic waters, or a combination of both. For instance, the water flow of River Severn, the longest river of the British Isles, shows decreasing flows from winter to summer and autumn [website, Open WIMS data]. The estimated zero-salinity endmember generally shows highest dTM concentrations in July and lowest values in November (Fig. S12), possibly reflecting seasonal variations of the zero-salinity endmember. This phenomenon can alternatively be explained by the enhanced influence of remineralization at stations away from the fluvial source, evidenced by the gradually increased subsurface nutrient concentrations at station CCS relative to other stations (Fig. S12). Therefore, the distributions of dTMs and nutrients as well as their correlations on the NE Atlantic continental shelf were balanced by sources and seasonal cycling of biogeochemical processes.

3.3 Water mass mixing drive metal:P kinks at depth

The waters on the NE Atlantic continental slope between the SML and ~ 1000 m are characterized by the presence of East North Atlantic Central Waters (ENACW), Mediterranean Outflow Waters (MOW), and Sub-Arctic Intermediate Waters (SAIW) (Fig. S13). The increasing percentage contribution of MOW with depth is accompanied by increasing dTM and nutrient concentrations. At depths of 950 – 1050 m with the highest MOW contribution (~ 60%), waters showed strongly elevated dAl (20.1 ± 1.5 nM) compared with shallow waters (Table S4). Waters below ~ 1000 m are characterized by a gradually decreasing MOW contribution, and increasing contributions of Labrador Sea Water (LSW) and North East Atlantic Deep Waters (NEADW) (Fig.

S13). The concentrations of dTMs and nutrients continuously increased with depth, showing dAl of ~ 18 nM, dCd of ~ 350 pM, dCu of ~ 2.2 nM, dNi of ~ 5 nM, dZn of ~ 2.7 nM in bottom waters (Table S2). These concentrations are similar to the reported deep dCd (310 ± 26 pM), dNi (4.1 ± 0.4 nM), and dCu (1.56 ± 0.33 nM) values for this region (Cotté-Krief et al., 2002) and consistent with reported deep water concentrations of dTMs and nutrients in the North Atlantic Ocean (Achterberg et al., 2021; Saager et al., 1997).

No apparent kinks were identified for ratios of dCd:P (261 μmol mol^{-1}), dNi:P (1.94 mmol mol^{-1}), and dZn:P (2.26 mmol mol^{-1}) in waters > 100 m (Table S3). The dCd:P ratio here is consistent with the dCd:P ratio (280 μmol mol^{-1}, at P 0.5 – 1.5 μM) from the north Atlantic Ocean (GEOTRACES Intermediate Data Product Group, 2021; Middag et al., 2018; Roshan & Wu, 2015) and the expected dCd:P ratio in the Atlantic Ocean using a Rayleigh model with a fractionation factor ($\alpha_{Cd/P}$) of 1.6 – 2 (Elderfield & Rickaby, 2000) (Fig. S14). The lack of dCd:P kink also agrees with the linear dCd-P relationship at P < 1.3 μmol kg^{-1} (de Baar et al., 1994; Cullen, 2006; Frew & Hunter, 1992; Middag et al., 2018). The dNi – P and dZn – P correlations here were similar to those reported for the North Atlantic Ocean with dNi:P of 2.01 mmol mol^{-1} dZn:P of 1.77 mmol mol^{-1} at P of 0.5 – 1.5 μM (Fig. S14) (GEOTRACES Intermediate Data Product Group, 2021). In contrast, the dCu:P ratio on the continental slope increased from 0.31 mmol mol^{-1} at 100 – 1000 m to 2.78 mmol mol^{-1} at depths > 1000 m and the dAl concentrations showed pronounced variations with increasing P levels. Considering the small variations of dCu concentrations in surface waters (Table S2) and that Al is not a bio-essential element, the occurrence of changes in dCu:P and dAl:P ratios should reflect physical (e.g., water mass mixing) rather than biological processes. The importance of water mass mixing on the distributions of deep-water dTMs and nutrients is further demonstrated by the significant positive loadings of dTMs, nutrients, depth, density, and AOU in the same principal component (RC1, 55.9% of total variance) when using principal component analysis (PCA) (Supporting information: PCA, Fig, S15).

Here, we estimated the elemental composition of each water mass using a three-step calculation (Table S4). (1) At depths < ~ 1000 m, endmember concentrations of MOW were calculated from the positive linear correlations with dTM concentrations as dTM levels decreased with increasing contributions of ENACW and SAIW (Fig. S16). (2) Then, the dTM (and nutrient) concentrations were corrected by removing the MOW contributions. At depths > ~ 1000 m, the

residual dTMs were contributed by LSW, NEADW, and SAIW, where the endmember SAIW concentrations were calculated from the significant negative linear relationship between corrected SAIW contribution and corrected dTM concentrations (Fig. S17). The endmember concentrations of NEADW were evaluated at LSW < 1% (corresponding depth of 1000 – 1500 m) (Fig. S18a). (3) Finally, the endmember concentrations of LSW and ENACW were estimated by removing the contributions of MOW, SAIW, and NEADW (Fig. S18b and c).

All dTMs and nutrients showed significant correlations with percentage contributions of LSW and ENACW at the final step, despite uncertainties propagating during each step in the calculations. The predicted dTM concentrations, reconstructed by direct multiplication of water mass fractions with their endmember values, illustrate almost identical values with the observed concentrations (Fig. S19) with very low residuals (Fig. S20). In addition, the estimated endmember dAl concentrations of MOW are consistent with the increased dAl concentrations of MOW due to the dissolution of atmospherically deposited Saharan dust in the Mediterranean Basin (dAl = 35.6 ± 6.8 nM) (Table S4) (GEOTRACES Intermediate Data Product Group, 2021; Measures et al., 2015; Rolison et al., 2015). The calculated endmember concentrations of NEADW agree with deep water (> 4000 m) concentrations in the NE Atlantic Ocean (GEOTRACES Intermediate Data Product Group, 2021; Liu & Tanhua, 2021), where NEADW is a persistent feature (van Aken, 2000a; García-Ibáñez et al., 2015, 2018; Reinthaler et al., 2013). Therefore, our estimations on the apparent endmember concentrations of each water mass are robust to show their relative chemical compositions.

The correlations between reconstructed dTMs and nutrients corresponded to the observed results, and no kinks were observed for the correlations between dCd, dNi, dZn, and P, while dCu:P and dAl:P ratios showed deflections at ~ 1000 m (Fig. 4). Furthermore, the dTM:AOU and nutrient:AOU ratios changed abruptly at depths of ~ 1000 m and ~ 2000 m across all seasons (Fig. S7), coinciding with the variations of water mass fractions from MOW+SAIW+ENACW at 100 – 1000 m to MOW+NEADW+LSW at > 1000 m. Therefore, the AOU variations at depths > 100 m mostly reflect physical processes (e.g., water mass mixing) rather than local biological processes. These observations indicate that the distributions of subsurface dTMs and nutrients and their ratios on the NE Atlantic continental margin are mainly controlled by the mixing of water masses driven by ocean circulation and local remineralization processes therefore make a

minor contribution.

3.4 The influence of MOW on the dTM distributions on the NE Atlantic Ocean

The appearances of dTM:nutrient and dTM:AOU kinks at ~ 1000 m and ~ 2000 m are closely related to the maximum and diminished occurrence of MOW (Fig. 4, Fig. S7), probably ascribed to the distinctive dTM and nutrient stoichiometry of MOW relative to other water masses (Table S2). For instance, MOW shows much higher dAl:P but lower dCu:P ratios than LSW and NEADW (Fig. S21), thus creating kinks of dCu:P and dAl:P ratios at the maximum occurrence of MOW. Therefore, MOW provides an important imprint on dTM distributions on the continental slope of the NE Atlantic Ocean.

The MOW is formed in the Mediterranean Sea and spreads across the NE Atlantic Ocean at ~ 500 – 1500 m towards the Bay of Biscay and further along the shelf break of Celtic Sea (van Aken, 2000b; Price et al., 1993). The occurrence of MOW in the NE Atlantic Ocean can be observed in elevated dAl concentrations and salinity (Measures et al., 2015; Middag et al., 2022; Rolison et al., 2015) at depths of 900 – 1400 m (Fig. S22). Similar to the long-distance transport of anthropogenic Pb from MOW to the NE Atlantic continental margin (Rusiecka et al., 2018), our results suggest that nutrient and dTM signals of MOW were transported from the Gibraltar channel to the NE Atlantic continental margin. The significant correlations between dTMs and salinity (Fig. S23) demonstrate that dTMs in the MOW core were predominantly controlled by the conservative isopycnal mixing between MOW and lower salinity water masses (e.g., SAIW with similar density range to MOW; Johnson & Gruber, 2007) during ocean circulation, rather than scavenging removal. Specifically, the dAl, dZn, and dNi concentrations of the MOW core decreased with decreasing salinity, suggesting the saline MOW is a net source to deliver Mediterranean-sourced Al, Zn, and Ni into the NE Atlantic Ocean (Middag et al., 2022).

Furthermore, the minor seasonal variations of dTMs and nutrients in the MOW core possibly reflect seasonal cycles of water mass circulation along the slope of the NE Atlantic continental margin. Due to the wind-driven processes (Roque et al., 2019), the influence of SAIW in the NE Atlantic Ocean declined in autumn. Hence, higher MOW signals (e.g., higher salinity) were observed along the continental slope in November with respect to April and July. Accordingly, the MOW core on the slope showed slightly higher dAl and dZn but lower dCd concentrations in

November than those in April and July (Fig. S23).

4. Conclusions

Our findings illustrate the seasonal variations of dTMs and nutrients in surface waters on the continental margin of the NE Atlantic Ocean. The surface dTM concentrations on the shelf were also influenced by a zero-salinity endmember, e.g., fluvial materials from the British Isles. Therefore, temperate shelf sea ecosystems can be influenced by local biological processes and external sources, where riverine inputs play an essential role to deliver terrestrial dTMs to the ocean. The dTM concentrations and metal:P ratios at depth in the slope region can be explained by mixing of water masses driven by ocean circulation without invoking local remineralization. Specifically, the long-distance transportation of MOW delivers Mediterranean-sourced dTMs (e.g., dAl, dZn, and Ni) into the NE Atlantic Ocean and drives dAl:P and dCu:P kinks at a depth of ~ 1000 m along the NE Atlantic continental margin. Future climate change driven changes in dust inputs into the Mediterranean and water mass characteristics in the subpolar gyre, therefore, will have consequences for nutrient stoichiometry and the biological carbon cycles in the NE Atlantic Ocean.

Acknowledgments

Data availability

Data are held at the British Oceanographic Data Centre (http://www.bodc.ac.uk/).

Author contributions:

References

Achterberg, E. P., Colombo, C., & van den Berg, C. M. G. (1999). The distribution of dissolved Cu, Zn, Ni, Co and Cr in English coastal surface waters. *Continental Shelf Research*, *19*(4), 537–558. https://doi.org/10.1016/S0278-4343(98)00093-4

Achterberg, E. P., Steigenberger, S., Klar, J. K., Browning, T. J., Marsay, C. M., Painter, S. C., et

al. (2021). Trace Element Biogeochemistry in the High-Latitude North Atlantic Ocean: Seasonal Variations and Volcanic Inputs. *Global Biogeochemical Cycles*, *35*(3), e2020GB006674. https://doi.org/10.1029/2020GB006674

van Aken, H. M. (2000a). The hydrography of the mid-latitude northeast Atlantic Ocean: I: The deep water masses. *Deep Sea Research Part I: Oceanographic Research Papers*, *47*(5), 757–788. https://doi.org/10.1016/S0967-0637(99)00092-8

van Aken, H. M. (2000b). The hydrography of the mid-latitude Northeast Atlantic Ocean: II: The intermediate water masses. *Deep Sea Research Part I: Oceanographic Research Papers*, *47*(5), 789–824. https://doi.org/10.1016/S0967-0637(99)00112-0

Anderson, L. A., & Sarmiento, J. L. (1994). Redfield ratios of remineralization determined by nutrient data analysis. *Global Biogeochemical Cycles*, *8*(1), 65–80. https://doi.org/10.1029/93GB03318

de Baar, H. J. W., Saager, P. M., Nolting, R. F., & van der Meer, J. (1994). Cadmium versus phosphate in the world ocean. *Marine Chemistry*, *46*(3), 261–281. https://doi.org/10.1016/0304-4203(94)90082-5

Baars, O., Abouchami, W., Galer, S. J. G., Boye, M., & Croot, P. L. (2014). Dissolved cadmium in the Southern Ocean: Distribution, speciation, and relation to phosphate. *Limnology and Oceanography*, *59*(2), 385–399. https://doi.org/10.4319/lo.2014.59.2.0385

Birchill, A. J., Milne, A., Woodward, E. M. S., Harris, C., Annett, A., Rusiecka, D., et al. (2017). Seasonal iron depletion in temperate shelf seas. *Geophysical Research Letters*, *44*(17), 8987–8996. https://doi.org/10.1002/2017GL073881

Boyd, P. W., Ellwood, M. J., Tagliabue, A., & Twining, B. S. (2017). Biotic and abiotic retention, recycling and remineralization of metals in the ocean. *Nature Geoscience*, *10*(3), 167–173. https://doi.org/10.1038/ngeo2876

Boyle, E. A., Sclater, F., & Edmond, J. M. (1976). On the marine geochemistry of cadmium. *Nature*, *263*(5572), 42–44. https://doi.org/10.1038/263042a0

Boyle, Edward A. (1988). Cadmium: Chemical tracer of deepwater paleoceanography. *Paleoceanography*, *3*(4), 471–489.

Bruland, K. W. (1992). Complexation of cadmium by natural organic ligands in the central North Pacific. *Limnology and Oceanography*, *37*(5), 1008–1017. https://doi.org/10.4319/lo.1992.37.5.1008

Bruland, K. W., Middag, R., & Lohan, M. C. (2014). Controls of Trace Metals in Seawater. In *Treatise on Geochemistry* (pp. 19–51). Elsevier. https://doi.org/10.1016/B978-0-08-095975-7.00602-1

Cotté-Krief, M.-H., Thomas, A. J., & Martin, J.-M. (2002). Trace metal (Cd, Cu, Ni and Pb) cycling in the upper water column near the shelf edge of the European continental margin (Celtic Sea). *Marine Chemistry*, *79*(1), 1–26. https://doi.org/10.1016/S0304-4203(02)00013-0

Cullen, J. T. (2006). On the nonlinear relationship between dissolved cadmium and phosphate in the modern global ocean: Could chronic iron limitation of phytoplankton growth cause the kink? *Limnology and Oceanography*, *51*(3), 1369–1380. https://doi.org/10.4319/lo.2006.51.3.1369

Cutter, G., Casciotti, K., Croot, P., Geibert, W., Heimbürger, L.-E., Lohan, M., et al. (2017). Sampling and Sample-handling Protocols for GEOTRACES Cruises. Version 3, August

2017. *GEOTRACES Standards and Intercalibration Committee*.

Elderfield, H., & Rickaby, R. E. M. (2000). Oceanic Cd/P ratio and nutrient utilization in the glacial Southern Ocean. *Nature*, *405*(6784), 305–310. https://doi.org/10.1038/35012507

Frew, R. D., & Hunter, K. A. (1992). Influence of Southern Ocean waters on the cadmium–phosphate properties of the global ocean. *Nature*, *360*(6400), 144–146. https://doi.org/10.1038/360144a0

García-Ibáñez, M. I., Pardo, P. C., Carracedo, L. I., Mercier, H., Lherminier, P., Ríos, A. F., & Pérez, F. F. (2015). Structure, transports and transformations of the water masses in the Atlantic Subpolar Gyre. *Progress in Oceanography*, *135*, 18–36. https://doi.org/10.1016/j.pocean.2015.03.009

García-Ibáñez, M. I., Pérez, F. F., Lherminier, P., Zunino, P., Mercier, H., & Tréguer, P. (2018). Water mass distributions and transports for the 2014 GEOVIDE cruise in the North Atlantic. *Biogeosciences*, *15*(7), 2075–2090. https://doi.org/10.5194/bg-15-2075-2018

GEOTRACES Intermediate Data Product Group. (2021). The GEOTRACES Intermediate Data Product 2021 (IDP2021). *NERC EDS British Oceanographic Data Centre NOC*. Retrieved from 10.5285/cf2d9ba9-d51d-3b7c-e053-8486abc0f5fd

Han, Q., Moore, J. K., Zender, C., Measures, C., & Hydes, D. (2008). Constraining oceanic dust deposition using surface ocean dissolved Al. *Global Biogeochemical Cycles*, *22*(2).

Ho, T.-Y., Quigg, A., Finkel, Z. V., Milligan, A. J., Wyman, K., Falkowski, P. G., & Morel, F. M. M. (2003). The Elemental Composition of Some Marine Phytoplankton1. *Journal of Phycology*, *39*(6), 1145–1159. https://doi.org/10.1111/j.0022-3646.2003.03-090.x

Horner, T. J., Lee, R. B. Y., Henderson, G. M., & Rickaby, R. E. M. (2013). Nonspecific uptake and homeostasis drive the oceanic cadmium cycle. *Proceedings of the National Academy of Sciences*, *110*(7), 2500–2505. https://doi.org/10.1073/pnas.1213857110

Hydes, D. J., & Liss, P. S. (1976). Fluorimetric method for the determination of low concentrations of dissolved aluminium in natural waters. *Analyst*, *101*(922), 922–931. https://doi.org/10.1039/an9760100922

Hydes, D. J., Aoyama, M., Aminot, A., Bakker, K., Becker, S., Coverly, S., & Daniel, A. (2010). Determination of dissolved nutrients (N, P, Si) in seawater with high precision and inter-comparability using gas-segmented continuous flow analysers. *In The GO-SHIP Repeat Hydrography Manual : A Collection of Expert Reports and Guidelines.*, *IOCCP No 1*(OCPO Publication Series No. 134, version 1), 1–87.

Janssen, D. J., Sieber, M., Ellwood, M. J., Conway, T. M., Barrett, P. M., Chen, X., et al. (2020). Trace metal and nutrient dynamics across broad biogeochemical gradients in the Indian and Pacific sectors of the Southern Ocean. *Marine Chemistry*, *221*, 103773. https://doi.org/10.1016/j.marchem.2020.103773

Johnson, G. C., & Gruber, N. (2007). Decadal water mass variations along 20°W in the Northeastern Atlantic Ocean. *Progress in Oceanography*, *73*(3), 277–295. https://doi.org/10.1016/j.pocean.2006.03.022

Kremling, K., & Hydes, D. (1988). Summer distribution of dissolved Al, Cd, Co, Cu, Mn and Ni in surface waters around the British Isles. *Continental Shelf Research*, *8*(1), 89–105. https://doi.org/10.1016/0278-4343(88)90026-X

Kremling, K., & Pohl, C. (1989). Studies on the Spatial and Seasonal Variability of Dissolved Cadmium , Copper and Nickel in North-, *27*, 43–60.

La Fontaine, S., Quinn, J. M., Nakamoto, S. S., Page, M. D., Göhre, V., Moseley, J. L., et al. (2002). Copper-dependent iron assimilation pathway in the model photosynthetic eukaryote Chlamydomonas reinhardtii. *Eukaryotic Cell*, *1*(5), 736–757.

Lane, T. W., & Morel, F. M. (2000). A biological function for cadmium in marine diatoms. *Proceedings of the National Academy of Sciences*, *97*(9), 4627–4631.

Lane, T. W., Saito, M. A., George, G. N., Pickering, I. J., Prince, R. C., & Morel, F. M. M. (2005). A cadmium enzyme from a marine diatom. *Nature*, *435*(7038), 42–42. https://doi.org/10.1038/435042a

Liu, M., & Tanhua, T. (2021). Water masses in the Atlantic Ocean: characteristics and distributions. *Ocean Science*, *17*(2), 463–486. https://doi.org/10.5194/os-17-463-2021

Lohan, M. C., & Tagliabue, A. (2018). Oceanic Micronutrients: Trace Metals that are Essential for Marine Life. *Elements*, *14*(6), 385–390. https://doi.org/10.2138/gselements.14.6.385

Mahaffey, C., Reynolds, S., Davis, C. E., & Lohan, M. C. (2014). Alkaline phosphatase activity in the subtropical ocean: insights from nutrient, dust and trace metal addition experiments. *Frontiers in Marine Science*, *1*, 73.

Measures, C., & Edmond, J. M. (1988). Aluminium as a tracer of the deep outflow from the Mediterranean. *Journal of Geophysical Research: Oceans*, *93*(C1), 591–595. https://doi.org/10.1029/JC093iC01p00591

Measures, C., Hatta, M., Fitzsimmons, J., & Morton, P. (2015). Dissolved Al in the zonal N Atlantic section of the US GEOTRACES 2010/2011 cruises and the importance of hydrothermal inputs. *Deep Sea Research Part II: Topical Studies in Oceanography*, *116*, 176–186. https://doi.org/10.1016/j.dsr2.2014.07.006

Menzel Barraqueta, J.-L., Schlosser, C., Planquette, H., Gourain, A., Cheize, M., Boutorh, J., et al. (2018). Aluminium in the North Atlantic Ocean and the Labrador Sea (GEOTRACES GA01 section): roles of continental inputs and biogenic particle removal. *Biogeosciences*, *15*(16), 5271–5286. https://doi.org/10.5194/bg-15-5271-2018

Middag, R., van Heuven, S. M. A. C., Bruland, K. W., & de Baar, H. J. W. (2018). The relationship between cadmium and phosphate in the Atlantic Ocean unravelled. *Earth and Planetary Science Letters*, *492*, 79–88. https://doi.org/10.1016/j.epsl.2018.03.046

Middag, R., Rolison, J. M., George, E., Gerringa, L. J. A., Rijkenberg, M. J. A., & Stirling, C. H. (2022). Basin scale distributions of dissolved manganese, nickel, zinc and cadmium in the Mediterranean Sea. *Marine Chemistry*, *238*, 104063. https://doi.org/10.1016/j.marchem.2021.104063

Moore, C. M., Mills, M. M., Arrigo, K. R., Berman-Frank, I., Bopp, L., Boyd, P. W., et al. (2013). Processes and patterns of oceanic nutrient limitation. *Nature Geoscience*, *6*(9), 701–710. https://doi.org/10.1038/ngeo1765

Moore, W. S. (2008). Fifteen years experience in measuring 224Ra and 223Ra by delayed-coincidence counting. *Marine Chemistry*, *109*(3–4), 188–197.

Morel, F. M. M., Reinfelder, J. R., Roberts, S. B., Chamberlain, C. P., Lee, J. G., & Yee, D. (1994). Zinc and carbon co-limitation of marine phytoplankton. *Nature*, *369*(6483), 740–742. https://doi.org/10.1038/369740a0

Morel, Francois M. M., & Price, N. M. (2003). The biogeochemical cycles of trace metals in the oceans. *Science*, *300*(5621), 944–947.

Muller-Karger, F. E., Varela, R., Thunell, R., Luerssen, R., Hu, C., & Walsh, J. J. (2005). The

484 importance of continental margins in the global carbon cycle. *Geophysical Research Letters*,
485 *32*(1), L01602.
486 Price, J. F., Baringer, M. O., Lueck, R. G., Johnson, G. C., Ambar, I., Parrilla, G., et al. (1993).
487 Mediterranean Outflow Mixing and Dynamics. *Science*, *259*(5099), 1277–1282.
488 https://doi.org/10.1126/science.259.5099.1277
489 Price, N. M., & Morel, F. M. M. (1990). Cadmium and cobalt substitution for zinc in a marine
490 diatom. *Nature*, *344*(6267), 658–660.
491 Rapp, I., Schlosser, C., Rusiecka, D., Gledhill, M., & Achterberg, E. P. (2017). Automated
492 preconcentration of Fe, Zn, Cu, Ni, Cd, Pb, Co, and Mn in seawater with analysis using high-
493 resolution sector field inductively-coupled plasma mass spectrometry. *Analytica Chimica*
494 *Acta*, *976*, 1–13. https://doi.org/10.1016/j.aca.2017.05.008
495 Reinthaler, T., Álvarez Salgado, X. A., Álvarez, M., van Aken, H. M., & Herndl, G. J. (2013).
496 Impact of water mass mixing on the biogeochemistry and microbiology of the Northeast
497 Atlantic Deep Water. *Global Biogeochemical Cycles*, *27*(4), 1151–1162.
498 https://doi.org/10.1002/2013GB004634
499 Rolison, J. M., Middag, R., Stirling, C. H., Rijkenberg, M. J. A., & de Baar, H. J. W. (2015). Zonal
500 distribution of dissolved aluminium in the Mediterranean Sea. *Marine Chemistry*, *177*, 87–
501 100. https://doi.org/10.1016/j.marchem.2015.05.001
502 Roque, D., Parras-Berrocal, I., Bruno, M., Sánchez-Leal, R., & Hernández-Molina, F. J. (2019).
503 Seasonal variability of intermediate water masses in the Gulf of Cádiz: implications of the
504 Antarctic and subarctic seesaw. *Ocean Science*, *15*(5), 1381–1397.
505 Roshan, S., & DeVries, T. (2021). Global Contrasts Between Oceanic Cycling of Cadmium and
506 Phosphate. *Global Biogeochemical Cycles*, *35*(6), e2021GB006952.
507 https://doi.org/10.1029/2021GB006952
508 Roshan, S., & Wu, J. (2015). Cadmium regeneration within the North Atlantic. *Global*
509 *Biogeochemical Cycles*, *29*(12), 2082–2094. https://doi.org/10.1002/2015GB005215
510 Rusiecka, D., Gledhill, M., Milne, A., Achterberg, E. P., Annett, A. L., Atkinson, S., et al. (2018).
511 Anthropogenic Signatures of Lead in the Northeast Atlantic. *Geophysical Research Letters*,
512 *45*(6), 2734–2743. https://doi.org/10.1002/2017GL076825
513 Saager, P. M., de Baar, H. J. W., de Jong, J. T. M., Nolting, R. F., & Schijf, J. (1997). Hydrography
514 and local sources of dissolved trace metals Mn, Ni, Cu, and Cd in the northeast Atlantic
515 Ocean. *Marine Chemistry*, *57*(3), 195–216. https://doi.org/10.1016/S0304-4203(97)00038-
516 8
517 Saito, M. A., Goepfert, T. J., Noble, A. E., Bertrand, E. M., Sedwick, P. N., & DiTullio, G. R.
518 (2010). A seasonal study of dissolved cobalt in the Ross Sea, Antarctica: micronutrient
519 behavior, absence of scavenging, and relationships with Zn, Cd, and P. *Biogeosciences*, *7*(12),
520 4059–4082. https://doi.org/10.5194/bg-7-4059-2010
521 Simpson, J. H., & Sharples, J. (2012). *Introduction to the physical and biological oceanography*
522 *of shelf seas*. Cambridge University Press.
523 Sunda, W. G., & Huntsman, S. A. (2000). Effect of Zn, Mn, and Fe on Cd accumulation in
524 phytoplankton: Implications for oceanic Cd cycling. *Limnology and Oceanography*, *45*(7),
525 1501–1516.
526 Twining, B. S., & Baines, S. B. (2013). The Trace Metal Composition of Marine Phytoplankton.
527 *Annual Review of Marine Science*, *5*(1), 191–215. https://doi.org/10.1146/annurev-marine-

121211-172322
Woodward, E. M. S., & Rees, A. P. (2001). Nutrient distributions in an anticyclonic eddy in the northeast Atlantic Ocean, with reference to nanomolar ammonium concentrations. *Deep Sea Research Part II: Topical Studies in Oceanography*, *48*(4), 775–793. https://doi.org/10.1016/S0967-0645(00)00097-7
Wu, J., & Roshan, S. (2015). Cadmium in the North Atlantic: Implication for global cadmium–phosphorus relationship. *Deep Sea Research Part II: Topical Studies in Oceanography*, *116*, 226–239. https://doi.org/10.1016/j.dsr2.2014.11.007
Wyatt, N. J., Milne, A., Woodward, E. M. S., Rees, A. P., Browning, T. J., Bouman, H. A., et al. (2014). Biogeochemical cycling of dissolved zinc along the GEOTRACES South Atlantic transect GA10 at 40°S. *Global Biogeochemical Cycles*, *28*(1), 44–56. https://doi.org/10.1002/2013GB004637
Xie, R. C., Galer, S. J., Abouchami, W., Rijkenberg, M. J., De Jong, J., De Baar, H. J., & Andreae, M. O. (2015). The cadmium–phosphate relationship in the western South Atlantic—The importance of mode and intermediate waters on the global systematics. *Marine Chemistry*, *177*, 110–123.
Zhang, J., Guo, X., & Zhao, L. (2019). Tracing external sources of nutrients in the East China Sea and evaluating their contributions to primary production. *Progress in Oceanography*, *176*, 102122. https://doi.org/10.1016/j.pocean.2019.102122

Figures

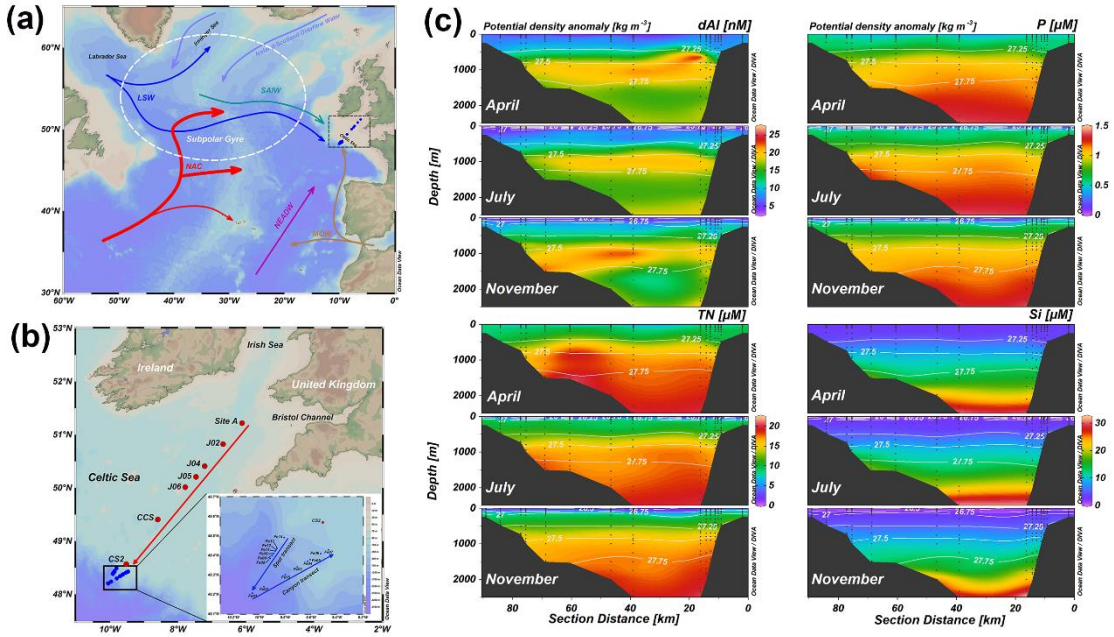

Fig. 1 (a) The schematic circulation of water masses (NAC: North Atlantic Current; LSW: Labrador Sea waters; SAIW: Sub-Arctic Intermediate Waters; MOW: Mediterranean Outflow Waters; NEADW: Northeast Atlantic Deep Waters) in the North Atlantic Ocean; (b) Sampling transects and locations on the Northeast Atlantic continental margin (Celtic Sea). The red and blue arrows define the shelf and slope sections, respectively, for Fig. 2 and Fig. 3. (c) Section plots of dissolved aluminum (dAl), phosphate (P), nitrate+nitrite (TN), and silicic acid (Si) along the slope transect during expeditions in November 2014 (DY018), April 2015 (DY029), and July 2015 (DY033) in Celtic Sea.

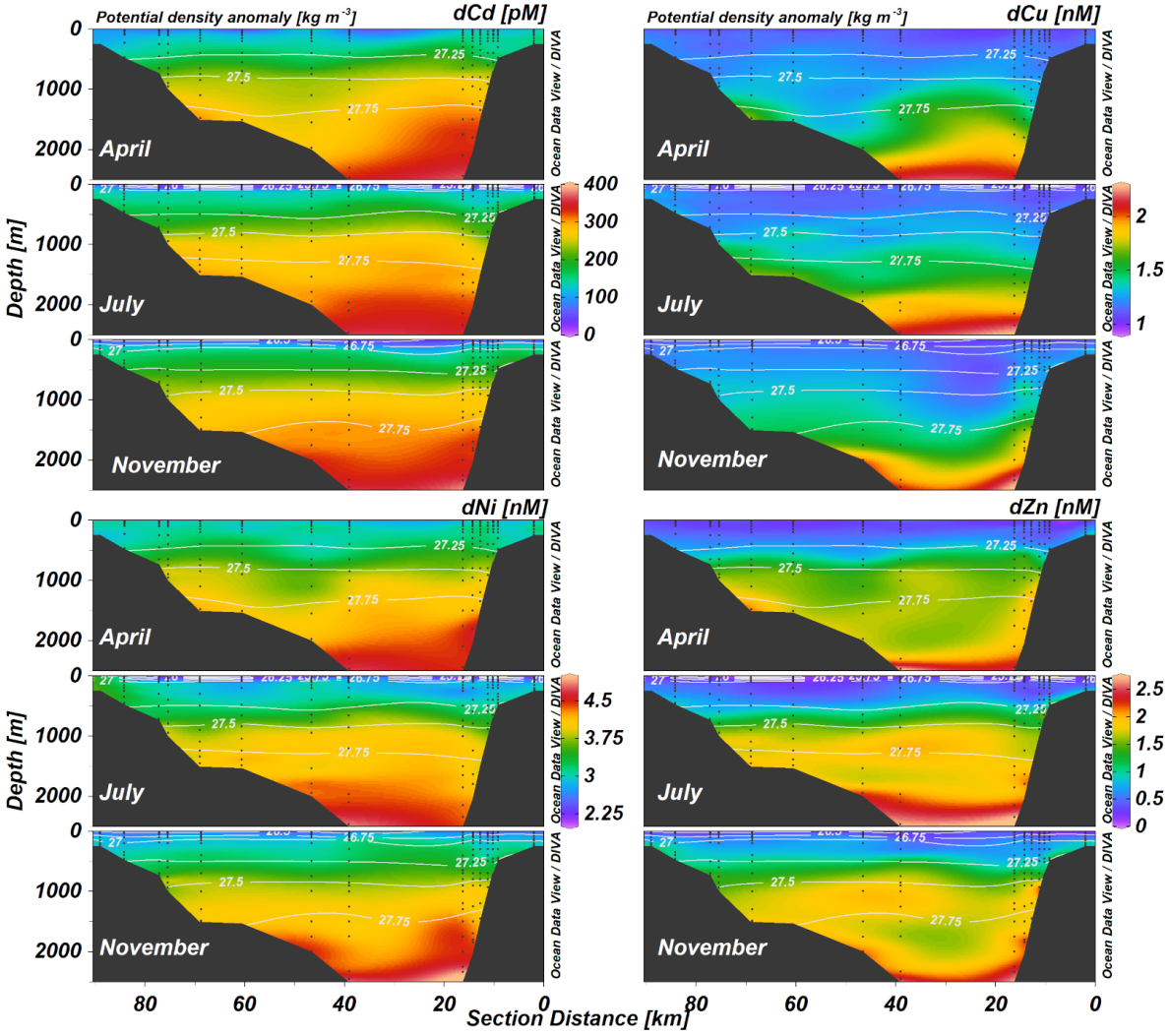

559

560 Fig. 2 Section plots of dissolved cadmium (dCd), copper (dCu), nickel (dNi), and zinc (dZn) on

561 the slope of the Northeast Atlantic continental margin. Samples were taken in November 2014,

562 April 2015, and July 2015, respectively. The section is defined in Fig. 1b.

563

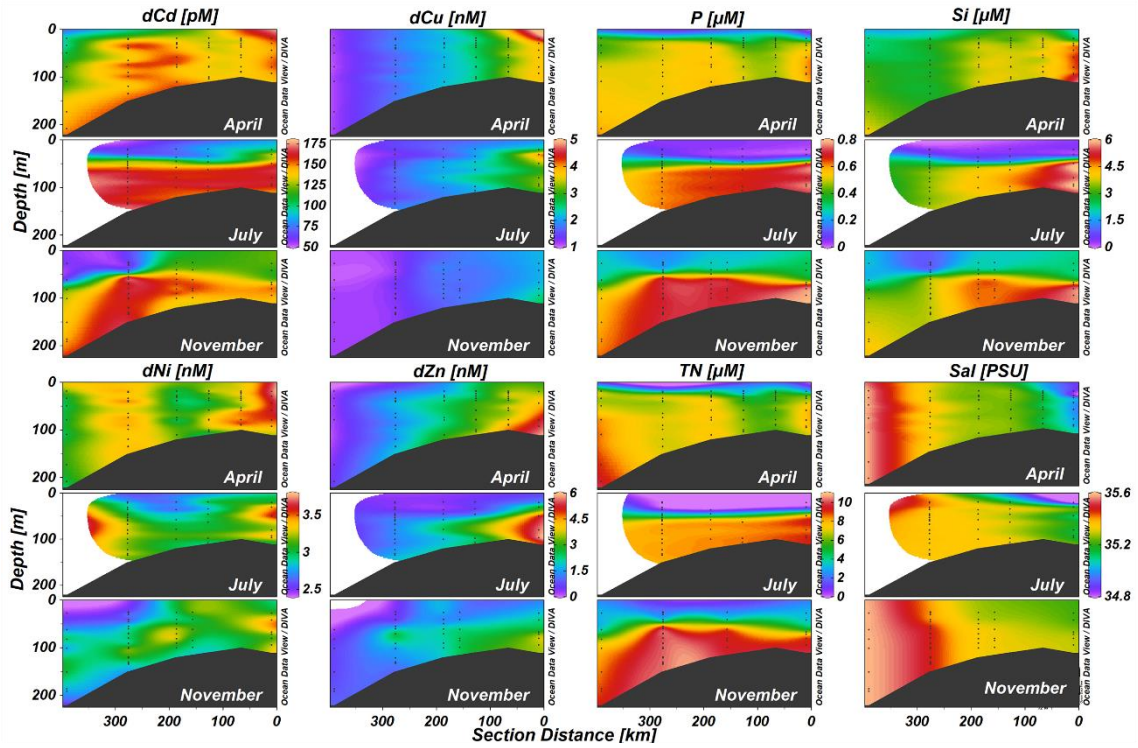

Fig. 3: Section plots of dissolved trace metals (dCd, dCu, dNi, dZn), salinity, and nutrients (nitrate+nitrite (TN), phosphate (P), silicic acid (Si)) on the continental shelf of the Northeast Atlantic Ocean. The section is defined in Fig. 1b. Samples were taken in November 2014, April 2015, and July 2015, respectively.

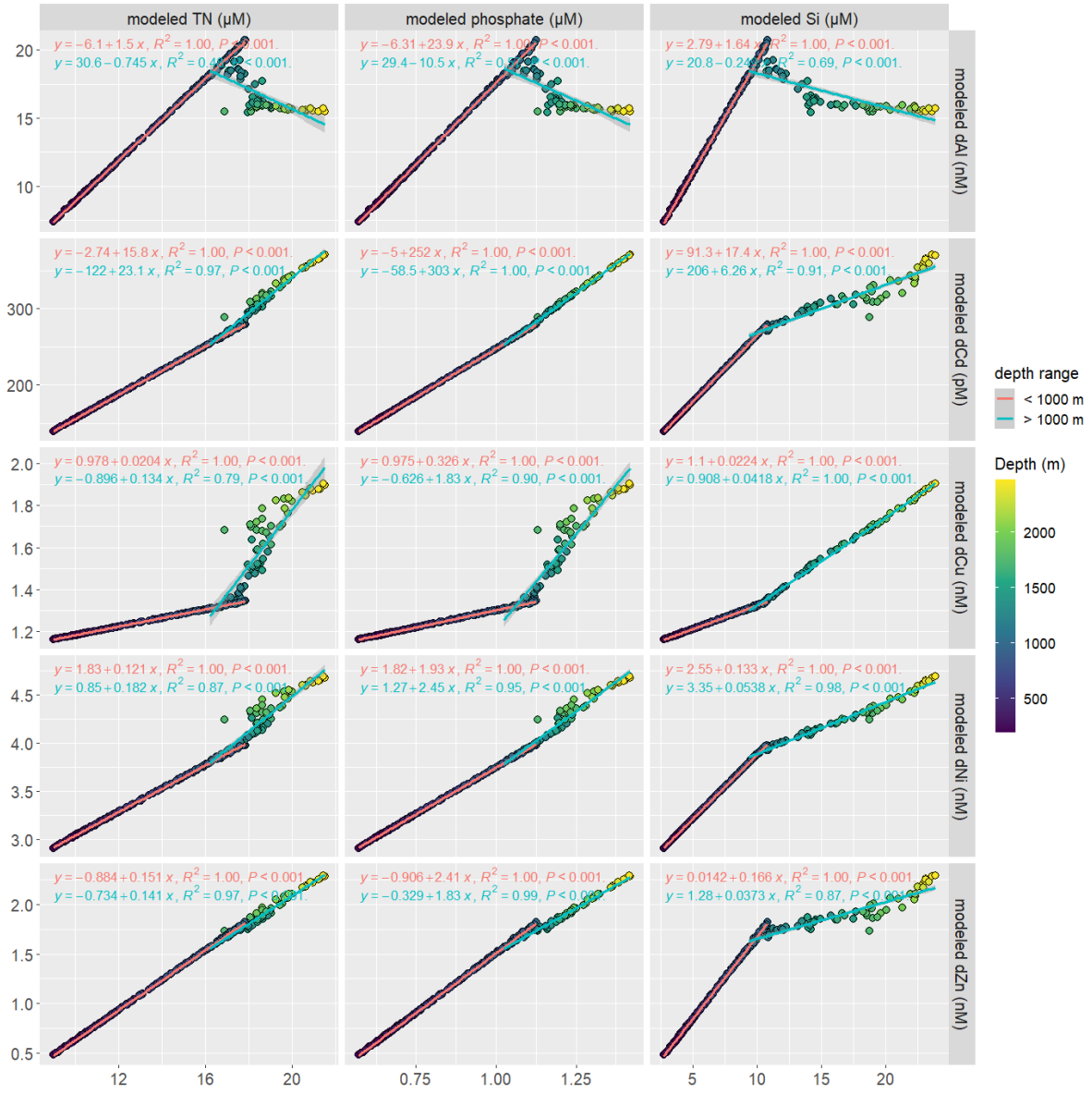

570

571 Fig. 4: Correlations between reconstructed dissolved trace metal (dTM: dAl, dCd, dCu, dNi, dZn)
572 and nutrient (nitrate+nitrite (TN), phosphate (P), and silicic acid (Si)) concentrations on the
573 Northeast Atlantic continental slope. Linear regression models were applied to depths < 1000 m
574 and depths > 1000 m, respectively.

575